

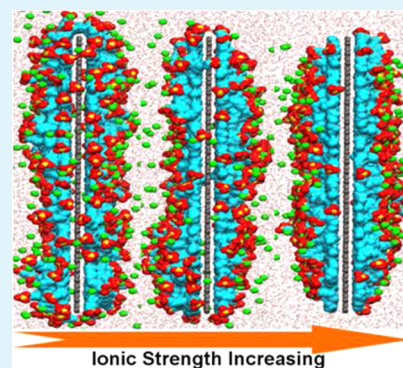
# Electrolyte-induced Reorganization of SDS Self-assembly on Graphene: A Molecular Simulation Study

Shuyan Liu, Bin Wu, and Xiaoning Yang\*

State Key Laboratory of Material-Orientated Chemical Engineering, College of Chemistry and Chemical Engineering, Nanjing University of Technology, Nanjing 210009, China

## Supporting Information

**ABSTRACT:** A molecular dynamics simulation was conducted to study the structure and morphology of sodium dodecyl sulfate (SDS) surfactants adsorbed on a nanoscale graphene nanostructure in the presence of an electrolyte. The self-assembly structure can be reorganized by the electrolyte-induced effect. An increase in the ionic strength of the added electrolyte can enhance the stretching of adsorbed surfactants toward the bulk aqueous phase and make headgroups assemble densely, leading to a more compact structure of the SDS/graphene composite. The change in the self-assembly structure is attributed to the accumulation/condensation of electrolyte cations near the surfactant aggregate, consequently screening the electrostatic repulsion between charged headgroups. The role of the electrolyte revealed here provides direct microscopic evidence or an explanation of the reported experiments in the electrolyte tuning of the interfacial structure of a surfactant aggregate on the surface of carbon nanoparticles. Additionally, the buoyant density of the SDS/graphene assembly has been computed. With an increase in the ionic strength of the electrolyte, the buoyant density of the SDS/graphene composite rises. The interfacial accumulation of electrolytes provides an important contribution to the density enhancement. The study will be valuable for the dispersion and application of graphene nanomaterials.



**KEYWORDS:** graphene, surfactant, self-assembly, molecular simulation, electrolyte, SDS

## 1. INTRODUCTION

Graphene has shown extensive applications in preparing new-type hybrid nanomaterials,<sup>1–4</sup> due to its excellent electronic, mechanical, thermal, and chemical properties.<sup>5–7</sup> In this aspect, surfactants self-assembled on the graphene surface can form structured aggregates, which are able to fabricate well controlled and ordered hybrid nanostructures, including metal/graphene<sup>8–10</sup> and metal-oxide/graphene nanocomposites.<sup>11–16</sup> The utilization of the surfactant not only solves the hydrophobic/hydrophilic incompatibility problem in nanocomposites but also acts as a molecular template to control the deposition and grafting of functional compounds on a nanoscale graphene surface.

For a long time, the effect of an electrolyte on the surfactant adsorption onto a solid surface has been experimentally studied.<sup>17–23</sup> Previous studies<sup>20,21</sup> have shown an increase in the adsorption amounts of ionic surfactants on a silica surface in the presence of electrolytes. This origin has been explained as the screening effect by electrolytes, which reduces the surfactant headgroup area and allows more tightly packed aggregates. Ducker and Lamont<sup>22</sup> found that, at the interface between muscovite mica and aqueous solution, more curved self-assembly structures of cationic surfactants were observed at higher electrolyte salt concentrations. It was also reported<sup>23</sup> that on macroscopic graphite the interaggregate spacing of adsorbed sodium dodecyl sulfate (SDS) molecules decreases as the NaCl concentration increases. Despite these efforts, at

present, studying the electrolyte effect on surfactant self-assembly structures onto solid surfaces still remains active.

In the recent research by Doorn et al.,<sup>24,25</sup> it was proposed that enhanced electrostatic screening on headgroups, originated from electrolyte addition, could induce an increased surface loading of sodium dodecyl sulfate (SDS) on a carbon nanotube (CNT) and a pronounced volume expansion in the SDS/CNT composite structure. Furthermore, fluorescence spectroscopy<sup>26</sup> and UV–vis–NIR absorbance experiments<sup>27</sup> have revealed that electrolyte-induced reorientation of the surfactant structure could eliminate several pockets of water from the tube surface. Additionally, it has been reported<sup>28</sup> that the electrolyte is able to modify the surfactant structure on CNT surfaces, leading to a change in the retention of SDS-suspended single-wall carbon nanotubes (SWNT) on agarose gels. However, the mechanism explanation was just obtained from indirect experimental deduction. It is highly essential to provide a direct molecular-level picture and analysis on the relevant microscopic structure and mechanism.

Understanding the electrolyte effect on the surfactant self-assembly structure on graphene nanosheets will improve graphene dispersion preparation and guide the design of novel graphene-based nanomaterials. If there is an analogy

Received: January 28, 2014

Accepted: March 26, 2014

Published: March 26, 2014

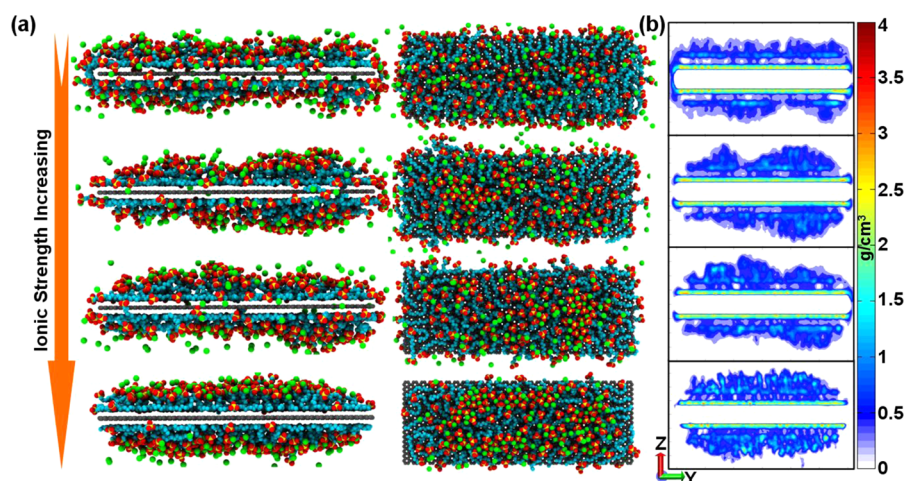


**Figure 1.** (a) Representative simulation snapshots of the SDS/graphene assembly structure obtained in the Full\_SDS system under four electrolyte solutions. From the top to the bottom: Pure aqueous solution, 0.6 M NaCl, 0.6 M CaCl<sub>2</sub>, 3.8 M CaCl<sub>2</sub>. Two views for each system: left is a side view; right is a front view. Color code: methyl groups, sulfur, and oxygen in SDS are represented by cyan, yellow, and red spheres, respectively. Sodium counterions are represented by green spheres. Carbon atoms in graphene are shown as black spheres. (b) Two-dimensional density distribution maps of SDS surfactants on the graphene surface.

between SWNT and graphene, it is expected that the electrolyte addition will result in the structural reorganization of adsorbed ionic surfactants on a graphene surface. This will not only modify the dispersion of graphene<sup>29–31</sup> but also provide an alternative to modulation of metal/graphene or metal-oxide/graphene nanohybrids.<sup>13–16</sup>

Molecular simulations have been performed to study the interfacial structure of surfactants on graphene surfaces.<sup>32–34</sup> Meanwhile, the effect of monovalent electrolytes on the morphology of surfactants on solid surfaces has been studied to some extent.<sup>27,35–37</sup> However, there is a lack of systematic studies of the effect of various electrolyte ions, including valence and concentration, on the structures and morphologies of ionic surfactants adsorbed on nanosized graphene sheets. With all of the above in mind, in the present study, we carried out an all-atomistic molecular dynamics (MD) simulation to study the self-assembly of SDS on a graphene surface in the presence of an electrolyte. The present study not only offers a systematic microscopic picture of the supermolecular surfactant/graphene nanostructure but also gives a comprehensive explanation on the function of electrolyte ions in the tuning of surfactant adsorption morphology.

## 2. METHODOLOGY

**2.1. Models and Simulation Details.** The carbon atoms in graphene were treated as uncharged Lennard-Jones (L-J) spheres.<sup>38</sup> These L-J potential parameters have been verified to be reasonable in simulating the carbon nanotube in water<sup>39</sup> and the SDS self-assembly on the CNT surface.<sup>40</sup> The potential parameters for SDS were adopted from the references 40 and 41, which have been successfully used to simulate the self-assembly of SDS molecules at the water/graphite interface<sup>41,42</sup> and the water/CNT interface.<sup>40</sup> Water molecules were represented by the SPC/E model.<sup>43</sup> The simulated parameters for the electrolyte ions (Na<sup>+</sup>, Mg<sup>2+</sup>, Ca<sup>2+</sup>, and Cl<sup>-</sup>) were obtained from the references 44–49, in which the microstructure of the aqueous ion–graphene interface has been simulated. For the van der Waals (vdW) interactions between different types of particles, the L-J potential with the Lorentz–Berthelot mixing rule was applied. However, for the water–graphene interaction, a carbon–oxygen L-J potential with the parameters from the work of Werder et al.<sup>50,51</sup> was used, which has been widely applied to simulate the contact angle of water droplets on a graphite surface.

The self-assembly MD simulations of SDS on graphene in electrolyte solutions were performed in the NPT ensemble using the Lammmps package.<sup>52</sup> All simulations were performed in the isothermal–isobaric ensemble (NPT), at a temperature of 300 K and pressure of 1.0 atm, with a time step of 2 fs and three-dimensional periodic boundary conditions. The particle mesh Ewald (PME) method<sup>53</sup> was used to calculate the long-range electrostatic interaction. Each graphene was considered to be a rigid body, and the carbon atoms at the edges were equally treated as the center atoms. As observed in Figure S1, there is no obvious difference in the simulation structures between rigid and flexible graphenes. This is consistent with previous studies.<sup>32,54</sup>

**2.2. Details on Initial Configuration and System Composition.** In this simulation, surfactants were initially placed on both sides of graphene with their axes perpendicular to the solid surface (defined as per-assembly initial configuration). This initial configuration has been used in the extensive simulations of SDS aggregates on graphites.<sup>41,42,55</sup> To verify the rationality, we additionally conducted simulations using another initial configuration, in which surfactant molecules were randomly distributed in the simulation cell (defined as the random initial configuration). It was demonstrated (Figure S2) that the same equilibrium self-assembly structures can be obtained using the two different initial configurations. This indicates that the simulation method in this work is reasonable. In general, MD simulation run with the random configuration was carried out for 200 ns, and the preassembly system was run for 40 ns. We used the last 10 ns trajectories collected per 1000 steps for the structure analysis.

Two surface coverages for SDS on the graphene surface were considered: one is 2.2 SDS molecules/nm<sup>2</sup> (45 Å<sup>2</sup>/molecule, denoted as the Full\_SDS system), corresponding to saturated surface coverage<sup>23,42,56</sup> on graphite; another is 1.0 SDS molecules/nm<sup>2</sup> (Low\_SDS), which is in good agreement with the monolayer adsorption model on the graphite surface.<sup>57</sup> Actually, the finite size of the graphene sheet has a certain effect on the morphology of surfactant aggregates.<sup>32,34</sup> However, the single-layer graphene sheet in this work is composed of 1960 carbon atoms with a size of 42 Å × 118 Å. Thus, the self-assembly structure and morphology under the two packing densities could reasonably represent the characteristics of SDS adsorption on nanosized graphene sheets. In this work, the main goal is to study the electrolyte effect on SDS adsorption onto graphene. It is expected that the simulation results obtained here should capture the important information. The electrolyte ions were added randomly, and various types and concentrations of electrolytes were investigated. The salt concentration presented here only includes the added electrolyte ions without considering the counterions SDS\_Na<sup>+</sup>. The detailed

simulation systems are listed in Table S1 in the Supporting Information.

### 3. RESULTS AND DISCUSSION

In this work, we carried out a series of MD simulations on SDS adsorption under different electrolyte conditions (total 28 systems, see Table S1). Figure 1 shows the representative simulation results in four typical electrolyte solutions. The equilibrium snapshots show that the tailgroups of surfactants are close to the graphene surface, while most of the headgroups are exposed to the surrounding aqueous phase. This self-assembly performance can enlarge the contact between the hydrophobic tail segments and graphene surface. The two-dimensional density profiles, which reflect the projections of the surfactant density around the graphene surface, are shown in Figure 1b. In pure aqueous solution, SDS surfactants adsorbed on the graphene surface form a rough multilayer structure, which agrees well with the previous simulation.<sup>32</sup> However, previous experiments<sup>23,58</sup> and simulations<sup>35,42,59,60</sup> showed that SDS could form a hemicylinder micelle on graphite when the surfactant concentration reached saturation. The difference is possible due to the finite surface size of the graphene nanosheet investigated in this work, which can result in the side edge adsorption behavior.<sup>32,34</sup>

It is observed that the existence of an electrolyte can have an obvious effect on the morphology of SDS micelles. With a monovalent or divalent electrolyte at a low concentration (0.6 M), adsorbed surfactants can form partial hemicylinder micelles. For 0.6 M NaCl, the imperfect hemicylinder morphology shows that the periodicity of the surfactant aggregates is about 50 Å, which is similar to the experimental observation of periodic SDS striations (~5.2 nm) on graphite surfaces.<sup>23,60</sup>

For 0.6 M divalent electrolyte CaCl<sub>2</sub>, the formed hemicylinder micelle becomes more curved. Furthermore, with 3.8 M CaCl<sub>2</sub>, the SDS molecules obviously display a complete smooth hemicylinder structure on graphene. As compared with the other three systems, the surfactants at 3.8 M CaCl<sub>2</sub> demonstrate enhanced stretching toward the aqueous phase, corresponding to a more compact self-assembly structure. The assembly structure is somewhat similar to the full-cylinder aggregate structure on the CNT surface reported in previous experiments<sup>61,62</sup> and simulations.<sup>63–65</sup> The enhanced extending degree of surfactant chains has also been observed for dodecyl sulfate adsorbed on CNTs when the sodium counterions (Na<sup>+</sup>) are substituted with Cs<sup>+</sup> ones.<sup>27</sup> Actually, the more vertical adsorption pattern of the surfactant relative to the surface might vacate additional adsorption space on the surface and could lead to a further increase in the adsorption amount of surfactants. Although this further adsorption cannot be observed in the present MD simulation with a finite number of surfactants placed on the graphene surface, this observation is in qualitative agreement with the previous hypothesis<sup>24,25</sup> that the volume expansion of the SDS/SWNT composite is caused by more surfactant adsorption with salt addition. Meanwhile, the more compactly packing manner of headgroups on the graphene surface can also be supported by the probability distribution of the minimal distance between the headgroups (in Figure S3). For other systems, similar self-assembly behavior has been observed (see Figure S4). To sum up, an increase in both valence and concentration of electrolyte ions, corresponding to an enhancement of the ionic strength of

the electrolyte, can improve the surfactant stretching and make surfactants pack more closely.

The interfacial density distributions of the tailgroups, headgroups, and sodium counterions of SDS are shown in Figure 2, as a function of the distance  $z$  perpendicular to the

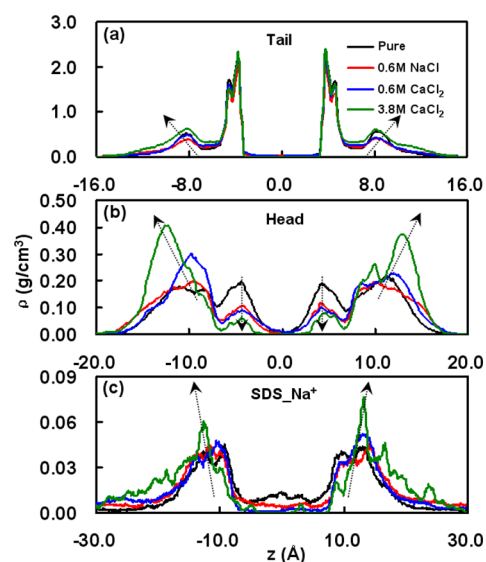


**Figure 2.** Density profiles of surfactant under four electrolyte solutions in the Full SDS system along the  $z$  axis perpendicular to the graphene surface. (a) tail segment, (b) headgroup, and (c) sodium counterion.

surface. The sharp first peaks in the density distributions of tailgroups (Figure 2a) indicate that most tailgroups remain in close contact with the surface. Increasing the ionic strength can result in an obvious shift of the headgroup density peak (Figure 2b) away from the graphene. This means more surfactant headgroups protruding toward the aqueous solution, increasing the extending degree of surfactants. The result is consistent with the previous simulation<sup>36</sup> that the density peaks of SDS headgroups on a macroscopic graphite surface become sharper, as the salt concentration increases.

On the basis of the density profiles of headgroups, the maximum height of the aggregate relative to the graphene surface is estimated to be 17.5 Å, which is in good agreement with the AFM experimental height value ( $17 \pm 0.5$  Å) for the SDS micelle on the graphite–solution interface.<sup>23</sup> We observe that some surfactant headgroups are located near the graphene surface, as shown by the first peak at  $\sim \pm 4$  Å in Figure 2b. This phenomenon is possible due to the side edge effect of the graphene nanosheet with finite surface size, which can keep headgroups clinging to the graphene edge.<sup>32,34</sup>

Figure 2c shows the density distribution of surfactant counterions, which can be considered as the counterion accumulation/condensation behavior near the headgroups.<sup>32,59,66,67</sup> The counterion condensation effect can also be observed in the snapshots (Figure 1), in which the counterions are located inside the micelle, just like being sandwiched between the SDS headgroups.<sup>32,66</sup> Similar density profiles for the electrolyte ions were presented in Figure S5. There also is an accumulation/condensation of electrolyte cations near the surfactant aggregate. These results demonstrate that the charged headgroups in the SDS aggregate can produce attractive interaction with the counterions and the electrolyte cations.

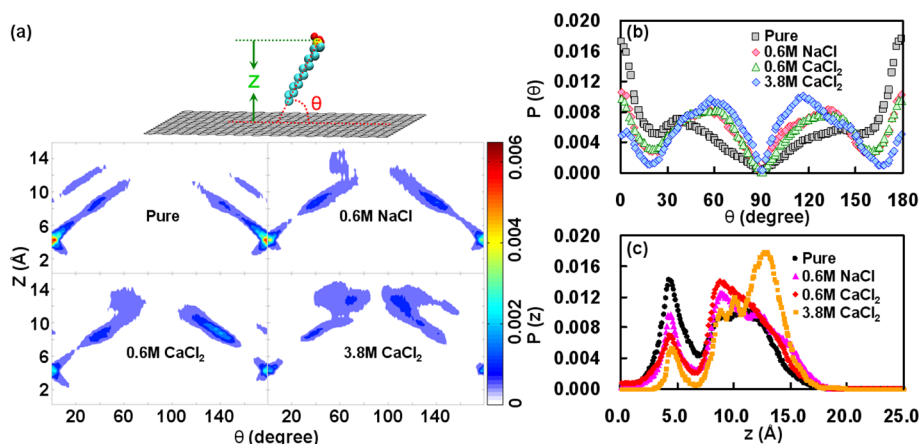


**Figure 3.** (a) Orientational distribution of surfactants in the Full\_SDS as a function of the separation ( $z$ , abscissa) between headgroups and the graphene surface.  $\theta$  represents the orientation angle between the principal axis of the SDS and the parallel vector with respect to the graphene plane under different separations,  $z$ . (b) Probability distribution of the average orientation angle between the principal axis of the SDS and the graphene surface. (c) The probability distributions of the height of surfactant headgroup relative to the graphene surface.

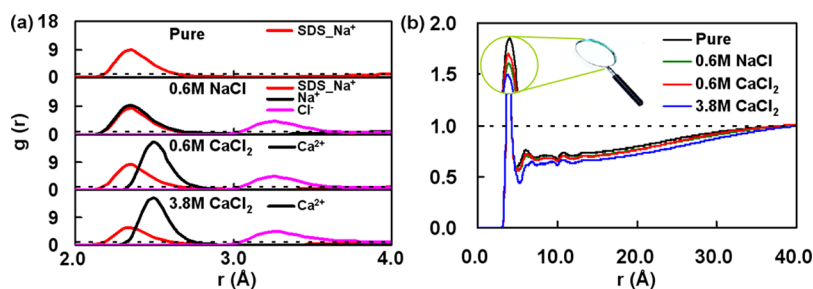


**Figure 4.** Radial distribution function ( $g(r)$ ) of the water molecules around (a) ions and (b) SDS headgroups in the Full\_SDS system. SDS\_Na<sup>+</sup> is the counterions of the surfactant, and Na<sup>+</sup> is the added electrolyte sodium ions.

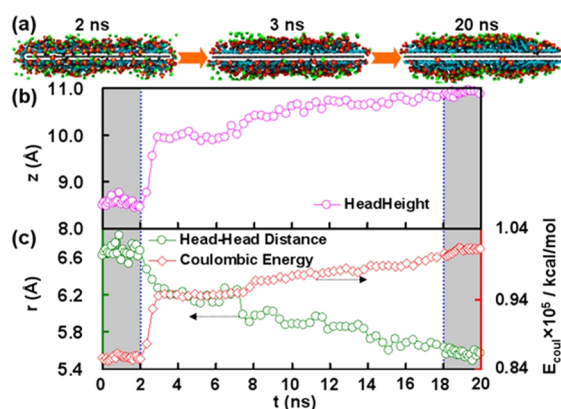
The orientation distribution of adsorbed SDS molecules has been shown in Figure 3a, where the orientation angle ( $\theta$ ) of the surfactant is correlated with its position ( $z$ ) in regard to the surface. In the pure SDS/graphene system without electrolytes, four strip bands in the angle distribution represent two layers of SDS assembly on the graphene surface. It is in accordance with the morphology observed in Figure 1. As the ionic strength increases, the orientation distribution curves are elongated and the distribution density becomes denser at the larger separation from the surface. This result indicates an increase in the perpendicular orientation of surfactants with the ionic strength, corresponding to an enhanced stretching of surfactant toward the aqueous phase. This behavior can be further supported by the probability distributions of the average orientation angle (Figure 3b) and the height of the surfactant headgroup relative to the graphene surface (Figure 3c).

Figure 4a shows the radial distribution functions (RDFs) between the ions and the solvent, which reveals that the water molecules solvate well to these ions.<sup>68</sup> An increase in the ionic strength can lead to a decrease in the RDF peak around the sodium counterions (SDS-Na<sup>+</sup>), meaning a decline in the local water structure around SDS\_Na<sup>+</sup>. This is consistent with the condensation effect of counterions with more SDS\_Na<sup>+</sup> ions binding to the headgroups (Figure 2c). This phenomenon can also be confirmed by the RDFs between the headgroups and the water molecules ( $g(r_{\text{O}_{\text{headgroup}}-\text{O}_{\text{Water}}}))$  in Figure 4b, where the intensity of first peaks becomes weaker with the ionic strength increasing.

According to the above result, the SDS surfactants demonstrate a more compact adsorption pattern in the CaCl<sub>2</sub> solution (3.8 M) with a preference of perpendicular orientation relative to the graphene surface. Next, we want to check if this enhanced stretching self-assembly morphology can be made through a structure transformation from other equilibrium configurations by adding an electrolyte. Herein, we performed a MD self-assembly simulation with the initial configuration, which was adopted from the final equilibrium structure in pure SDS/graphene aqueous solution (without additional electrolyte). The electrolyte CaCl<sub>2</sub> (3.8 M) was then added in the simulation system, and we monitor the dynamical process of SDS self-assembly on graphene.

The representative process snapshots are presented in Figure 5a. During the initial stage (0–2 ns), the equilibrium MD run was performed for the pure aqueous SDS/graphene system (Full\_SDS) without added electrolyte, and the multilayer structure of surfactants on the graphene surface can keep stable. After a simulation time of 3 ns, i.e., 1 ns after the introduction of additional CaCl<sub>2</sub> electrolyte, the surfactant aggregate begins to rearrange its structure. In a period of time, the micelle morphology can reorganize into rough hemicylindrical structure with more surfactants extending to the aqueous phase. After 20 ns, a steady complete hemicylinder structure has been formed. A detailed comparison of the equilibrium structures of SDS/graphene aggregates is shown in Figure S6.

In Figure 5b, as expected, the average height of the surfactant headgroup, relative to the graphene surface, increases as a function of the simulation time. Meanwhile, the time evolution



**Figure 5.** (a) Snapshots of SDS assembly on the graphene surface. The time evolution of (b) the average height of surfactant headgroup relative to the graphene surface and (c) the Coulombic energy between SDS headgroups and the average minimal distance between them.

of the Coulombic energy between SDS headgroups and the average minimal distance between headgroups is presented in Figure 5c. The increase in the Coulombic energy between charged headgroups and the reduction of the minimal distance further illustrate that the electrolyte can strengthen the screening effect on the electrostatic repulsion between headgroups, thereby making adjacent headgroups contact more closely. This screening effect is mainly associated with the binding interaction of the added electrolyte cations with the surfactant headgroups.

Additionally, the surfactant self-assembly on the graphene surface (Low\_SDS) under low packing density was also simulated. The equilibrium snapshots and the corresponding two-dimensional projection densities of the SDS/graphene aggregation are shown in Figure 6. In the absence of added electrolyte, the SDS molecules form a sparse disordered monolayer structure with the surfactants lying along the graphene surface. This is similar to previous simulations on surfactant adsorbed on CNT<sup>40,67</sup> and the graphite surface.<sup>55,59,69</sup> With an increase in the ionic strength, a similar extending behavior for surfactant adsorption morphology is observed (see Figures S7–S11). However, the stretching degree of SDS for the Low\_SDS system is relatively weak.

Figure 7 shows a straight quantitative correlation between the change of surfactant structures and the ionic strength of

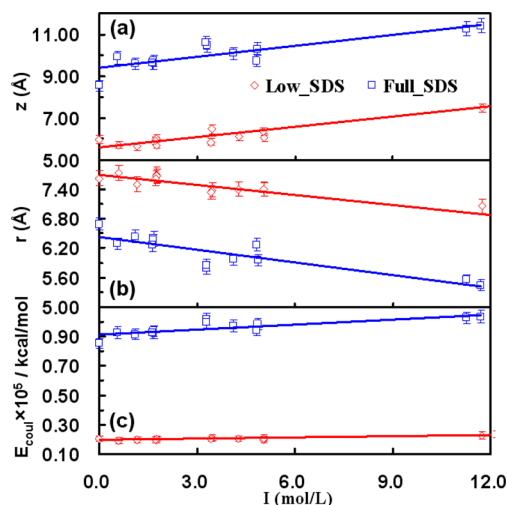


**Figure 7.** (a) The average height of surfactant headgroup relative to graphene surface. (b) The average minimal distance between headgroups. (c) The Coulombic energy between headgroups as a function of electrolyte ionic strength. The solid line is the relevant linear fitting.

electrolytes for all 28 investigated systems. Herein, the ionic strengths were calculated only based on the introduced electrolyte ions in the aqueous solution without considering the sodium counterions (SDS Na<sup>+</sup>). With ionic strength increasing, there is a rise in the average surfactant height, a reduction in the minimal distance between headgroups, and an increase in the Coulombic repulsive energy between negatively charged headgroups. This result confirms the formation of a compact structure of the SDS/graphene assembly with electrolyte addition and further reflects the electrolyte-induced effect.

From the above result, the added electrolyte ions can screen the electrostatic repulsion between negatively charged headgroups, consequently leading to an enhanced stretching of surfactant chains toward the aqueous phase. This reorganization of self-assembly structures of adsorbed surfactants is expected to result in an increase in the steric repulsion between

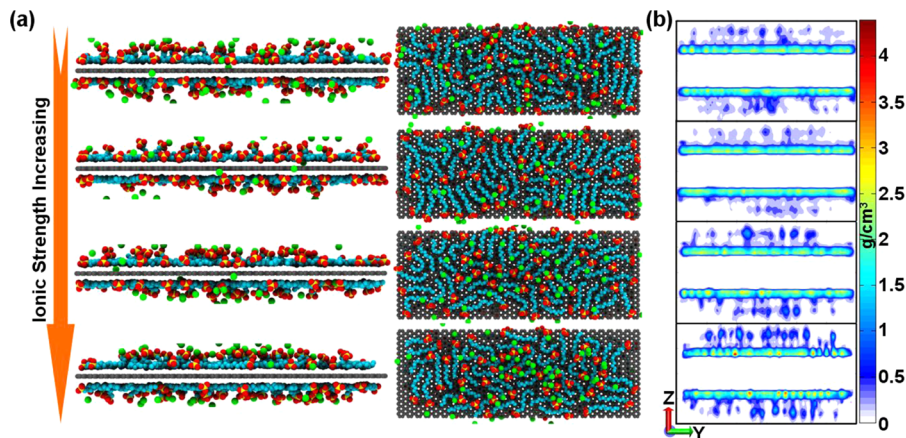


**Figure 6.** Same as in Figure 1 but for the Low\_SDS system. (a) Representative simulation snapshots of the SDS/graphene assembly structure. (b) Two-dimensional density distribution maps of SDS surfactants on the graphene surface.

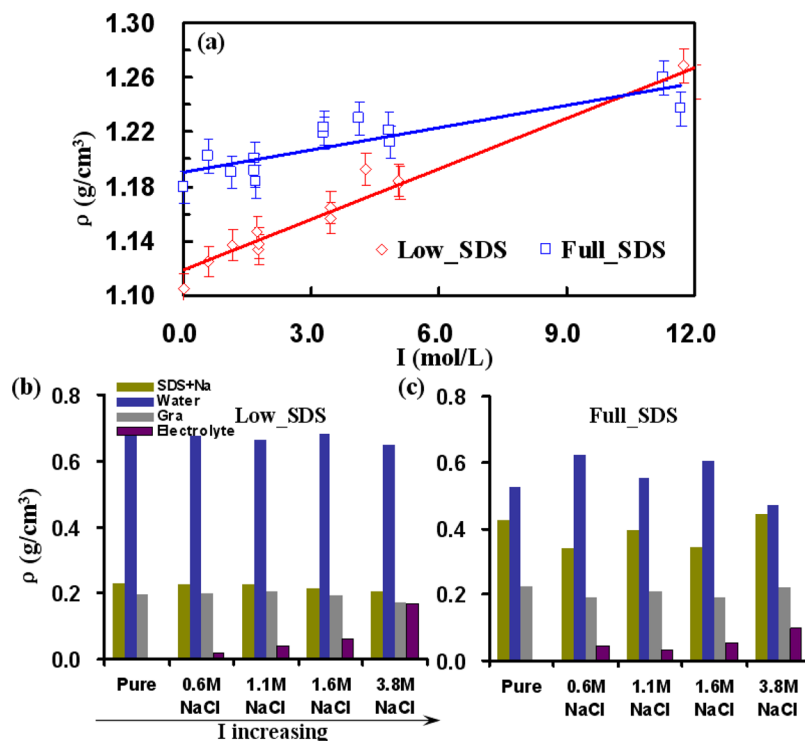


**Figure 8.** (a) Density of graphene-SDS assembly ( $\rho_{\text{Gra-SDS}}$ ) as a function of the ionic strength of the electrolyte (open symbol) and the fitted curve (solid line, that is only a guide for the eyes). The decomposition of the total density into the various contributions for the NaCl electrolyte in (b) Low\_SDS and (c) Full\_SDS systems.

individual SDS/graphene assemblies. Our simulation might provide a molecular-level support that controlling the ionic strength of the electrolyte can help with tuning the interfacial interaction between surfactant-coated graphene sheets, which is highly valuable in surfactant-stabilized graphene dispersion and preparation.<sup>29</sup> In addition, our simulation suggests that the rearrangement of surfactant self-assembly under various electrolyte conditions could provide a method to modulate the hybrid template for effective deposition of metal or metal oxide on nanoscale graphene surfaces.

Recent research<sup>30</sup> has shown that ultracentrifuging graphene nanosheets stabilized by surfactants is a promising route for achieving the desired separation. The self-assembly structure of surfactant adsorbed on the graphene surface might determine the effective buoyant density of the aggregate,<sup>67,70</sup> which is the key factor in the ultracentrifuging separation of graphene. As discussed above, the electrolyte can change the SDS assembly structure on graphene. Therefore, it is very necessary to further evaluate the effect of the electrolyte on the buoyant density of SDS/graphene assembly.

The complex density of the SDS/graphene assembly,  $\rho_{\text{Gra-SDS}}$ , was calculated by integrating the total density of species along the  $z$  axis as follows:<sup>33</sup>

$$\rho_{\text{Gra-SDS}} = \frac{1}{z_2 - z_1} \int_{z_1}^{z_2} (\rho_{\text{Gra}} + \rho_{\text{SDS-Na}^+} + \rho_{\text{Electrolyte}} + \rho_{\text{Water}}) dz \quad (1)$$

where the integration boundary ( $Z_1$  and  $Z_2$ ) is chosen based on the positions where the water density reaches its bulk value. For all systems investigated in this work, the integration extremes in eq 1 used the same values with  $Z_1 = -16.5 \text{ \AA}$  and  $Z_2 = 16.5 \text{ \AA}$ .

Figure 8a depicts the densities of graphene-SDS assembly as a function of electrolyte ionic strengths for the two systems (Low\_SDS and Full\_SDS). On the whole, the complex densities for the Full\_SDS system are higher than those for the Low\_SDS system. In the pure SDS solution without electrolyte, the simulated density of the graphene-SDS assembly for the Full\_SDS system is equal to  $\sim 1.18 \text{ g/cm}^3$ , which is close to the experimental buoyant density ( $1.16 \text{ g/cm}^3$ ) of the graphene-sodium cholate surfactant assembly.<sup>30</sup>

As shown in Figure 8a, the assembly densities increase as the ionic strength rises. It is observed that the increasing degree of density in the Low\_SDS system is larger than that in the Full\_SDS system. In order to explain the possible origin, we decomposed the total density into various contributions. Figure 8b and c show the decomposition for the case of a NaCl electrolyte, and other systems are shown in Figures S12 and S13. These results indicate that the interfacial water molecules make a significant contribution to the density of the supramolecular assembly.

For the SDS/graphene assembly, the increase in the density with the ionic strength is mainly caused by the presence of an electrolyte. Although a change in the aggregate morphology corresponds to a structure expansion, which might lead to a decrease of the aggregate density, the interfacial accumulation of electrolytes near the SDS aggregate provides an overwhelming impact on the density change. In the Low\_SDS system, the electrolyte can produce a more obvious influence on the complex density with the ionic strength increasing. It is possible due to the fact that under higher surface coverage of the surfactant there is no vacating room for electrolyte occupation.

## 4. CONCLUSION

Molecular dynamics simulations have been performed to study the effect of electrolyte on the aggregate morphology and self-assembly structure of SDS surfactants adsorbed on a nanoscale graphene surface. It is observed that the self-assembly structure of adsorbed surfactants can be reorganized by electrolyte addition. An increase of electrolyte ionic strength can lead to a transformation of the surfactant morphology from a rough multilayer disordered structure to a hemicylindrical structure, corresponding to a more compact morphology of the SDS/graphene composite. These molecular-level pictures are consistent with current experiments and simulations on surfactant adsorption on carbon surfaces. This behavior can be interpreted in terms of the enhanced screening effect on the electrostatic repulsion between headgroups, which is ascribed to the so-called cation condensation/accumulation near the surfactant headgroups. This simulated result provides, on the molecular level, insight into new routes for controlling the interfacial structures and forces for surfactant/graphene assemblies, which is valuable for the preparation and application of graphene-based nanomaterials.

The buoyant density of the SDS/graphene assembly has been calculated. This result shows that the interfacial solvent molecules make a major contribution to the density of the supramolecular assembly. With an increase in the ionic strength, the density rises due to the contribution of electrolyte binding. The change in the buoyant density might enhance and optimize the density gradient separation (DGS) approach in the graphene dispersion with controlled thickness.<sup>30,31</sup>

## ■ ASSOCIATED CONTENT

### Supporting Information

A list of simulated systems and some supporting figures. This material is available free of charge via the Internet at <http://pubs.acs.org>.

## ■ AUTHOR INFORMATION

### Corresponding Author

\*E-mail: [Yangxia@njtech.edu.cn](mailto:Yangxia@njtech.edu.cn).

### Notes

The authors declare no competing financial interest.

## ■ ACKNOWLEDGMENTS

This work was supported by the National Natural Science Foundation of China under Grant 21176114 and A PAPD Project of Jiangsu Higher Education Institution.

## ■ REFERENCES

- (1) Stankovich, S.; Dikin, D. A.; Dommett, G. H. B.; Kohlhaas, K. M.; Zimney, E. J.; Stach, E. A.; Piner, R. D.; Nguyen, S. T.; Ruoff, R. S. Graphene-based Composite Materials. *Nature* **2006**, *442*, 282–286.
- (2) Peak, S. M.; Yoo, E. J.; Honma, I. Enhanced Cyclic Performance and Lithium Storage Capacity of SnO<sub>2</sub>/graphene Nanoporous Electrodes with Three-dimensionally Delaminated Flexible Structure. *Nano Lett.* **2009**, *9*, 72–75.
- (3) Wang, X. R.; Tabakman, S. M.; Dai, H. J. Atomic Layer Deposition of Metal Oxides on Pristine and Functionalized Graphene. *J. Am. Chem. Soc.* **2008**, *130*, 8152–8153.
- (4) Qu, L. T.; Liu, Y.; Baek, J. B.; Dai, L. M. Nitrogen-doped Graphene as Efficient Metal-free Electrocatalyst for Oxygen Reduction in Fuel Cells. *ACS Nano* **2010**, *4*, 1321–1326.

- (5) Novoselov, K. S.; Geim, A. K.; Morozov, S. V.; Jiang, D.; Zhang, Y.; Dubonos, S. V.; Grigorieva, I. V.; Firsov, A. A. Electric Field Effect in Atomically Thin Carbon Films. *Science* **2004**, *306*, 666–669.

- (6) Novoselov, K. S.; Jiang, D.; Schedin, F.; Booth, T. J.; Khotkevich, V. V.; Morozov, S. V.; Geim, A. K. Two-dimensional Atomic Crystals. *Proc. Natl. Acad. Sci. U. S. A.* **2005**, *102*, 10451–10453.

- (7) Geim, A. K.; Novoselov, K. S. The Rise of Graphene. *Nat. Mater.* **2007**, *6*, 183–191.

- (8) Li, Y.; Fan, X. B.; Qi, J. J.; Ji, J. Y.; Wang, S. L.; Zhang, G. L.; Zhuang, F. B. Gold Nanoparticles–graphene Hybrids as Active Catalysts for Suzuki Reaction. *Mater. Res. Bull.* **2010**, *45*, 1413–1418.

- (9) Xiang, J. L.; Drzal, L. T. Electron and Phonon Transport in Au Nanoparticle Decorated Graphene Nanoplatelet Nanostructured Paper. *ACS Appl. Mater. Interfaces* **2011**, *3*, 1325–1332.

- (10) Vadukumpully, S.; Gupta, J.; Zhang, Y. P.; Xu, G. Q.; Valiyaveetil, S. Functionalization of Surfactant Wrapped Graphene Nanosheets with Alkylazides for Enhanced Dispersibility. *Nanoscale* **2011**, *3*, 303–308.

- (11) Wu, J. C.; Shi, W. W.; Chopra, N. Synthesis and Characterization of Graphene–mesoporous Silica Nanoparticle Hybrids. *J. Phys. Chem. C* **2012**, *116*, 12861–12874.

- (12) Wang, D. H.; Choi, D. W.; Li, J.; Yang, Z. G.; Nie, Z. M.; Kou, R.; Hu, D. H.; Wang, C. M.; Saraf, L.; Zhang, J. G.; Aksay, I. A.; Liu, J. Self-assembled TiO<sub>2</sub>–graphene Hybrid Nanostructures for Enhanced Li-ion Insertion. *ACS Nano* **2009**, *3*, 907–914.

- (13) Su, Y. Z.; Li, S.; Wu, D. Q.; Zhang, F.; Liang, H. W.; Gao, P. F.; Cheng, C.; Feng, X. L. Two-dimensional Carbon-coated Graphene/metal Oxide Hybrids for Enhanced Lithium Storage. *ACS Nano* **2012**, *6*, 8349–8356.

- (14) Wang, D. H.; Kou, R.; Choi, D. W.; Yang, Z. G.; Nie, Z. M.; Li, J.; Saraf, L. V.; Hu, D. H.; Zhang, J. G.; Graff, G. L.; Liu, J.; Pope, M. A.; Aksay, I. A. Ternary Self-assembly of Ordered Metal Oxide-graphene Nanocomposites for Electrochemical Energy Storage. *ACS Nano* **2010**, *4*, 1587–1595.

- (15) Wang, L. Q.; Wang, D. H.; Liu, J.; Exarhos, G. J. Probing Porosity and Pore Interconnectivity in Self-assembled TiO<sub>2</sub>-graphene Hybrid Nanostructures Using Hyperpolarized <sup>129</sup>Xe NMR. *J. Phys. Chem. C* **2012**, *116*, 22–29.

- (16) Xin, X.; Zhou, X. F.; Wu, J. H.; Yao, X. Y.; Liu, Z. P. Scalable Synthesis of TiO<sub>2</sub>/graphene Nanostructured Composite with High-rate Performance for Lithium Ion Batteries. *ACS Nano* **2012**, *6*, 11035–11043.

- (17) Stienstedt, J.; Froberg, J. C.; Tiberg, F.; Rutland, M. W. Forces between Silica Surfaces with Adsorbed Cationic Surfactants: Influence of Salt and Added Nonionic Surfactants. *Langmuir* **2005**, *21*, 1875–1883.

- (18) Imanishi, A.; Suzuki, M.; Nakato, Y. In Situ AFM Studies on Self-assembled Monolayers of Adsorbed Surfactant Molecules on Well-defined H-terminated Si(111) Surfaces in Aqueous Solutions. *Langmuir* **2007**, *23*, 12966–12972.

- (19) Mohr, A.; Nylander, T.; Piculell, L.; Lindman, B.; Boyko, V.; Bartels, F. W.; Liu, Y. Q.; Kurkal-Siebert, V. Mixtures of Cationic Copolymers and Oppositely Charged Surfactants: Effect of Polymer Charge Density and Ionic Strength on the Adsorption Behavior at the Silica–aqueous Interface. *ACS Appl. Mater. Interfaces* **2012**, *4*, 1500–1511.

- (20) Atkin, R.; Craig, V. S. J.; Biggs, S. Adsorption Kinetics and Structural Arrangements of Cationic Surfactants on Silica Surfaces. *Langmuir* **2000**, *16*, 9374–9380.

- (21) Lokar, W. J.; Ducker, W. A. Proximal Adsorption of Dodecyltrimethylammonium Bromide to the Silica–electrolyte Solution Interface. *Langmuir* **2002**, *18*, 3167–3175.

- (22) Lamont, R. E.; Ducker, W. A. Surface-induced Transformations for Surfactant Aggregates. *J. Am. Chem. Soc.* **1998**, *120*, 7602–7607.

- (23) Wanless, E. J.; Ducker, W. A. Organization of Sodium Dodecyl Sulfate at the Graphite–solution Interface. *J. Phys. Chem.* **1996**, *100*, 3207–3214.

- (24) Niyogi, S.; Densmore, C. G.; Doorn, S. K. Electrolyte Tuning of Surfactant Interfacial Behavior for Enhanced Density-based Separation

tions of Single-walled Carbon Nanotubes. *J. Am. Chem. Soc.* **2009**, *131*, 1144–1153.

(25) Duque, J. G.; Densmore, C. G.; Doorn, S. K. Saturation of Surfactant Structure at the Single-walled Carbon Nanotube Surface. *J. Am. Chem. Soc.* **2010**, *132*, 16165–16175.

(26) Duque, J. G.; Oudjedi, L.; Crochet, J. J.; Tretiak, S.; Lounis, B.; Doorn, S. K.; Cognet, L. Mechanism of Electrolyte-induced Brightening in Single-wall Carbon Nanotubes. *J. Am. Chem. Soc.* **2013**, *135*, 3379–3382.

(27) Suttipong, M.; Tummala, N. R.; Striolo, A.; Batista, C. S.; Fagan, J. Salt-specific Effects in Aqueous Dispersions of Carbon Nanotubes. *Soft Matter* **2013**, *9*, 3712–3719.

(28) Silvera-Batista, C. A.; Scott, D. C.; McLeod, S. M.; Ziegler, K. J. A Mechanistic Study of the Selective Retention of SDS-suspended Single-wall Carbon Nanotubes on Agarose Gels. *J. Phys. Chem. C* **2011**, *115*, 9361–9369.

(29) Lotya, M.; Hernandez, Y.; King, P. J.; Smith, R. J.; Nicolosi, V.; Karlsson, L. S.; Blighe, F. M.; De, S.; Wang, Z.; McGovern, L. T.; Duesberg, G. S.; Coleman, J. N. Liquid Phase Production of Graphene by Exfoliation of Graphite in Surfactant/water Solutions. *J. Am. Chem. Soc.* **2009**, *131*, 3611–3620.

(30) Green, A. A.; Hersam, M. C. Solution Phase Production of Graphene with Controlled Thickness via Density Differentiation. *Nano Lett.* **2009**, *9*, 4031–4036.

(31) Green, A. A.; Hersam, M. C. Emerging Methods for Producing Monodisperse Graphene Dispersions. *J. Phys. Chem. Lett.* **2009**, *1*, 544–549.

(32) Tummala, N. R.; Grady, B. P.; Striolo, A. Lateral Confinement Effects on the Structural Properties of Surfactant Aggregates: SDS on Graphene. *Phys. Chem. Chem. Phys.* **2010**, *12*, 13137–13143.

(33) Lin, S. C.; Shih, C. J.; Strano, M. S.; Blankschtein, D. Molecular Insights into the Surface Morphology, Layering Structure, and Aggregation Kinetics of Surfactant-stabilized Graphene Dispersions. *J. Am. Chem. Soc.* **2011**, *133*, 12810–12823.

(34) Wu, D.; Yang, X. N. Coarse-grained Molecular Simulation of Self-assembly for Nonionic Surfactants on Graphene Nanostructures. *J. Phys. Chem. B* **2012**, *116*, 12048–12056.

(35) Tummala, N. R.; Striolo, A. Role of Counterion Condensation in the Self-assembly of SDS Surfactants at the Water-graphite Interface. *J. Phys. Chem. B* **2008**, *112*, 1987–2000.

(36) Dominguez, H. Structure of the Sodium Dodecyl Sulfate Surfactant on a Solid Surface in Different NaCl Solutions. *Langmuir* **2009**, *25*, 9006–9011.

(37) Tummala, N. R.; Shi, L.; Striolo, A. Molecular Dynamics Simulations of Surfactants at the Silica–water Interface: Anionic vs Nonionic Headgroups. *J. Colloid Interface Sci.* **2011**, *362*, 135–143.

(38) Rappe, A. K.; Casewit, C. J.; Colwell, K. S.; Goddard, W. A.; Skiff, W. M. UFF, a Full Periodic Table Force Field for Molecular Mechanics and Molecular Dynamics Simulations. *J. Am. Chem. Soc.* **1992**, *114*, 10024–10035.

(39) Walther, J. H.; Jaffe, R.; Halicioglu, T.; Koumoutsakos, P. Carbon Nanotubes in Water: Structural Characteristics and Energetics. *J. Phys. Chem. B* **2001**, *105*, 9980–9987.

(40) Xu, Z. J.; Yang, X. N.; Yang, Z. A Molecular Simulation Probing of Structure and Interaction for Supramolecular Sodium Dodecyl Sulfate/single-wall Carbon Nanotube Assemblies. *Nano Lett.* **2010**, *10*, 985–991.

(41) Tummala, N. R.; Striolo, A. Role of Counterion Condensation in the Self-assembly of SDS Surfactants at the Water-graphite Interface. *J. Phys. Chem. B* **2008**, *112*, 1987–2000.

(42) Dominguez, H. Self-aggregation of the SDS Surfactant at a Solid-liquid Interface. *J. Phys. Chem. B* **2007**, *111*, 4054–4059.

(43) Berendsen, H. J. C.; Grigera, J. R.; Straatsma, T. P. The Missing Term in Effective Pair Potentials. *J. Phys. Chem.* **1987**, *91*, 6269–6271.

(44) Schweighofer, K. J.; Essmann, U.; Berkowitz, M. Simulation of Sodium Dodecyl Sulfate at the Water-vapor and Water-carbon Tetrachloride Interfaces at Low Surface Coverage. *J. Phys. Chem. B* **1997**, *101*, 3793–3799.

(45) Dominguez, H.; Rivera, M. Mixtures of Sodium Dodecyl Sulfate/dodecanol at the Air/water Interface by Computer Simulations. *Langmuir* **2005**, *21*, 7257–7262.

(46) Guardia, E.; Sese, G.; Padro, J. A.; Kalko, S. G. Molecular Dynamics Simulation of Mg<sup>2+</sup> and Ca<sup>2+</sup> Ions in Water. *J. Solution Chem.* **1999**, *28*, 1113–1126.

(47) Zhu, Y.; Lu, X. H.; Ding, H.; Wang, Y. R. Hydration and Association of Alkaline Earth Metal Chloride Aqueous Solution under Supercritical Condition. *Mol. Simul.* **2003**, *29*, 767–772.

(48) Predota, M.; Zhang, Z.; Fenter, P.; Wesolowski, D. J.; Cummings, P. T. Electric Double Layer at the Rutile (110) Surface.2. Adsorption of Ions from Molecular Dynamics and X-ray Experiments. *J. Phys. Chem. B* **2004**, *108*, 12061–12072.

(49) Chialvo, A. A.; Cummings, P. T. Aqua Ions-graphene Interfacial and Confinement Behavior: Insights from Isobaric-isothermal Molecular Dynamics. *J. Phys. Chem. A* **2011**, *115*, 5918–5927.

(50) Werder, T.; Walther, J. H.; Jaffe, R. L.; Halicioglu, T.; Koumoutsakos, P. On the Water-carbon Interaction for Use in Molecular Dynamics Simulations of Graphite and Carbon Nanotubes. *J. Phys. Chem. B* **2003**, *107*, 1345–1352.

(51) Zimmerli, U.; Gonnet, P. G.; Walther, J. H.; Koumoutsakos, P. Curvature Induced Defects in Water Conduction in Carbon Nanotubes. *Nano Lett.* **2005**, *5*, 1017–1022.

(52) Plimpton, S. Fast Parallel Algorithms for Short-range Molecular Dynamics. *J. Comput. Phys.* **1995**, *117*, 1–19.

(53) Darden, T.; York, D.; Pedersen, L. The Effect of Longrange Electrostatic Interactions in Simulations of Macromolecular Crystals: A Comparison of the Ewald and Truncated List Methods. *J. Chem. Phys.* **1993**, *99*, 8345–8348.

(54) Titov, A. V.; Kral, P.; Pearson, R. Sandwiched Graphene-membrane Superstructures. *ACS Nano* **2010**, *4*, 229–234.

(55) Sammalkorpi, M.; Panagiotopoulos, A. Z.; Haataja, M. Structure and Dynamics of Surfactant and Hydrocarbon Aggregates on Graphite: A Molecular Dynamics Simulation Study. *J. Phys. Chem. B* **2008**, *112*, 2915–2921.

(56) Bandyopadhyay, S.; Shelley, J. C.; Tarek, M.; Moore, P. B.; Klein, M. L. Surfactant Aggregation at a Hydrophobic Surface. *J. Phys. Chem. B* **1998**, *102*, 6318–6322.

(57) Kiraly, Z.; Findenegg, G. H. Calorimetric Evidence of the Formation of Half-cylindrical Aggregates of a Cationic Surfactant at the Graphite/water Interface. *J. Phys. Chem. B* **1998**, *102*, 1203–1211.

(58) Paruchuri, V. K.; Nalaskowski, J.; Shah, D. O.; Miller, J. D. The Effect of Cosurfactants on Sodium Dodecyl Sulfate Micellar Structures at a Graphite Surface. *Colloids Surf., A* **2006**, *272*, 157–163.

(59) Tummala, N. R.; Striolo, A. Curvature Effects on the Adsorption of Aqueous Sodium-dodecyl-sulfate Surfactants on Carbonaceous Substrates: Structural Features and Counterion Dynamics. *Phys. Rev. E* **2009**, *80*, 021408.

(60) Dominguez, H. Structural Transition of the Sodium Dodecyl Sulfate (SDS) Surfactant Induced by Changes in Surfactant Concentrations. *J. Phys. Chem. B* **2011**, *115*, 12422–12428.

(61) O'Connell, M. J.; Bachilo, S. M.; Huffman, C. B.; Moore, V. C.; Strano, M. S.; Haroz, E. H.; Rialon, K. L.; Boul, P. J.; Noon, W. H.; Kittrell, C.; Ma, J. P.; Hauge, R. H.; Weisman, R. B.; Smalley, R. E. Band Gap Fluorescence from Individual Single-walled Carbon Nanotubes. *Science* **2002**, *297*, 593–596.

(62) Richard, C.; Balavoine, F.; Schultz, P.; Ebbesen, T. W.; Mioskowski, C. Supramolecular Self-assembly of Lipid Derivatives on Carbon Nanotubes. *Science* **2003**, *300*, 775–778.

(63) Wallace, E. J.; Sansom, M. S. P. Carbon Nanotube Self-assembly with Lipids and Detergent: A Molecular Dynamics Study. *Nanotechnology* **2009**, *20*, 045101.

(64) Wallace, E. J.; Sansom, M. S. P. Carbon Nanotube/detergent Interactions via Coarse-grained Molecular Dynamics. *Nano Lett.* **2007**, *7*, 1923–1928.

(65) Duan, W. H.; Wang, Q.; Collins, F. Dispersion of Carbon Nanotubes with SDS Surfactants: A study from a Binding Energy Perspective. *Chem. Sci.* **2011**, *2*, 1407–1413.



- (66) Suttipong, M.; Tummala, N. R.; Kitiyanan, B.; Striolo, A. Role of Surfactant Molecular Structure on Self-assembly: Aqueous SDBS on Carbon Nanotubes. *J. Phys. Chem. C* **2011**, *115*, 17286–17296.
- (67) Tummala, N. R.; Striolo, A. SDS Surfactants on Carbon Nanotubes: Aggregate Morphology. *ACS Nano* **2009**, *3*, 595–602.
- (68) Zangi, R.; Hagen, M.; Berne, B. J. Effect of Ions on the Hydrophobic Interaction between Two Plates. *J. Am. Chem. Soc.* **2007**, *129*, 4678–4686.
- (69) Sammalkorpi, M.; Panagiotopoulos, A. Z.; Haataja, M. Surfactant and Hydrocarbon Aggregates on Defective Graphite Surface: Structure and Dynamics. *J. Phys. Chem. B* **2008**, *112*, 12954–12961.
- (70) Carvalho, E. J. F.; Dos Santos, M. C. Role of Surfactants in Carbon Nanotubes Density Gradient Separation. *ACS Nano* **2010**, *4*, 765–769.